

SOC-MartNet: A Martingale Neural Network for the Hamilton-Jacobi-Bellman Equation without Explicit $\inf_{u \in U} H$ in Stochastic Optimal Controls *

Wei Cai [†] Shuixin Fang [‡] Tao Zhou [§]

Abstract

In this work, we propose a martingale based neural network, SOC-MartNet, for solving high-dimensional Hamilton-Jacobi-Bellman (HJB) equations where no explicit expression is needed for the Hamiltonian $\inf_{u \in U} H(t, x, u, z, p)$, and stochastic optimal control problems with controls on both drift and volatility. We reformulate the HJB equations for the value function into a stochastic neural network learning process, i.e., training a control network and a value network such that the associated Hamiltonian process is minimized and the cost process becomes a martingale, yielding the value function. To enforce the martingale property for the cost process, we employ an adversarial network and construct a loss function based on the projection property of conditional expectations. Then, the control/value networks and the adversarial network are trained adversarially, such that the cost process is driven towards a martingale and the minimum principle is satisfied for the control. Numerical results show that the proposed SOC-MartNet is effective and efficient for solving HJB-type equations and SOCP with a dimension up to 1000 in a small number (less than 150) of training epochs.

Keywords: Hamilton-Jacobi-Bellman equation; high dimensional PDE; stochastic optimal control; adversarial networks; martingale method.

1 Introduction

This paper is devoted to the numerical solution of high-dimensional Hamilton-Jacobi-Bellman (HJB)-type equations and their applications to stochastic optimal control problems (SOCPs). The considered HJB-type equation is given in form of

$$\partial_t v(t, x) + \mathcal{L}v(t, x) + \inf_{\kappa \in U} H(t, x, \kappa, \partial_x v(t, x), \partial_{xx}^2 v(t, x)) = 0, \quad (t, x) \in [0, T] \times \mathbb{R}^d \quad (1)$$

*This work of SF and TZ is supported by the NSF of China (under grant 12288201) and the Youth Innovation Promotion Association (CAS). Date. July 8, 2024. *Previous version of this manuscript is published on arxiv arXiv:2405.03169, May 6, 2024*

[†]Department of Mathematics, Southern Methodist University, Dallas, TX 75275, USA. Email: cai@smu.edu. Corresponding author.

[‡]Institute of Computational Mathematics and Scientific/Engineering Computing, Academy of Mathematics and Systems Science, Chinese Academy of Sciences, Beijing, 100190, P. R. China. Email: sxfang@amss.ac.cn.

[§]Institute of Computational Mathematics and Scientific/Engineering Computing, Academy of Mathematics and Systems Science, Chinese Academy of Sciences, Beijing, 100190, P. R. China. Email: tzhou@lsec.cc.ac.cn. Corresponding author.

with $\partial_x = \nabla_x$ and $\partial_{xx}^2 = \nabla_x \nabla_x^\top$ as the gradient and Hessian operator, respectively, and a terminal condition

$$v(T, x) = g(x), \quad x \in \mathbb{R}^d, \quad (2)$$

where $U \subset \mathbb{R}^m$ and \mathcal{L} is a differential operator given by

$$\mathcal{L} := \mu(t, x) \partial_x + \frac{1}{2} \text{Tr} \left\{ \sigma \sigma^\top (t, x) \partial_{xx}^2 \right\}$$

for some given functions $\mu : [0, T] \times \mathbb{R}^d \rightarrow \mathbb{R}^d$ and $\sigma : [0, T] \times \mathbb{R}^d \rightarrow \mathbb{R}^{d \times q}$; $H(t, x, \kappa, z, p)$ is the Hamiltonian as a mapping $(t, x, \kappa, z, p) \in [0, T] \times \mathbb{R}^d \times U \times \mathbb{R}^d \times \mathbb{R}^{d \times d} \rightarrow \mathbb{R}$. The HJB-type equation (1) is general and covers common HJB equations appearing in SOCPs; see the discussions in section 3. Beyond this equation, this paper also explores the application of the proposed method to common semi-linear parabolic equations without boundary conditions.

The HJB equation is a fundamental partial differential equation (PDE) in the field of optimal control theory [43; 48]. In the typical framework of dynamic programming [5; 16; 35], the optimal feedback control is identified by the verification technique, which involves minimizing a Hamiltonian depending on the derivatives of a value function [48, p. 278]. On this account, the HJB equation, which governs this value function, stands as a cornerstone of dynamic programming. The well-posedness of HJB equations has been firmly established with the theory of viscosity solutions; see, e.g., [9; 10; 26; 27; 38]. But solving the HJB equation is still challenging due to its non-smoothness and high dimensionality.

The wide application of HJB equations has spurred extensive research on efficient numerical methods. Conventional approaches include the Galerkin method [3; 4; 46], the finite volume method [42; 45; 47], the monotone approximation scheme [2], the patchy dynamic programming [6; 40], etc. These methods generally suffer from the curse of dimensionality (CoD) [5], that is, the computation complexity increases exponentially with the dimension of the HJB equations. In [31; 32], the HJB equation is solved through the associated BSDE deduced from the Feynman-Kac representation [33]. However in their works, the resolution of BSDE relies on least-squares regressions, whose performance is still hampered by the curse of dimensionality. There are also literature leveraging dimension reduction techniques, e.g., [13; 29; 30; 37], but these techniques depend on the dimensionality reducibility of the problem.

In recent years, deep learning has emerged as a promising tool to overcome the CoD, leading to a growing body of deep learning methods for solving PDEs, e.g., [14; 15; 19; 21; 23; 25; 44; 49; 50]. While demonstrably effective for usual high-dimensional PDEs, these methods encounter new challenges when applied to the HJB-type equation (1). The main challenge stems from the inherent infimum operator in the Hamiltonian $\inf_{\kappa \in U}$ of HJB equation imposed on the H . Directly minimizing the Hamiltonian for every time-space point (t, x) is computationally expensive, a CoD problem itself.

To avoid this issue, the works in [11; 12; 23] focus on Hamilton-Jacobi equation where $\inf_{\kappa \in U} H$ is explicitly known. The work [39, section 3.4] considers specific optimal control problems such that $\inf_{\kappa \in U} H$ admits an analytic solution. There are also research resorting to neural networks. For example, [28, section 3.2] introduces a neural network to learn the feedback control $u(t, x)$ such that $u(t, x)$ becomes a stationary point of H , i.e., $\partial_\kappa H|_{\kappa=u(t, x)} = 0$, where certain conditions on U and H are needed to ensure the

stationary point is a minimizer of $\kappa \mapsto H$. The paper [52] considers static HJB-type PDEs, where solving $\inf_{\kappa \in U} H$ is avoided by reformulating the problem into a SOCP solved by reinforcement learning. In addition, there are also works on numerical methods for SOCPs, which do not explicitly solve the HJB equation, e.g., [1; 17; 20; 22; 24; 51]. By now, developing new efficient numerical methods for high-dimensional HJB equations still remains a actively researched topic.

In this paper, we propose a novel numerical method for solving the high-dimensional HJB-type equation (1). In our approach, the control and value functions of the problem are approximated by neural networks. The HJB equation is encoded into a Hamiltonian process and a cost process both depending on the control network and the value network. Then, the value and the control functions are found by minimizing a functional of the Hamiltonian process while ensuring the cost process is a martingale, which ensures the value function is found as the solution to the HJB equation. The martingale property is enforced by an adversarial learning, whose loss function is constructed by characterizing the projection property of conditional expectations. The proposed method, named SOC-MartNet, is able to solve stochastic optimal control problems based on the martingale formulation originally used in the DeepMartNet for boundary value and eigenvalue problems of high dimensional PDEs [7; 8]. Our numerical experiments will show that the proposed SOC-MartNet is effective and efficient for solving equations with dimension up to 1000.

The SOC-MartNet enjoys high computational efficiency stemming from the martingale formulation. In our approach, the task of finding $\inf_{\kappa \in U} H$ for each (t, x) is accomplished by training a control network to minimize a functional of the Hamiltonian process, thus avoiding the need of evaluating explicitly the infimum in the HJB equation. Moreover, our training algorithm enjoys parallel efficiency, since it is free of time-directed iterations during gradient computation. This feature is dramatically different from existing deep-learning probabilistic methods for PDEs. Beyond efficiency, the SOC-MartNet demonstrates broad applicability, effectively handling high-dimensional HJB equations and parabolic equations as well as SOCPs.

The remainder of this paper is organized as follows. In section 2, we briefly review the main ideas in dynamic programming for solving SOCPs. In section 3, we propose the SOC-MartNet and its algorithm for general non-degenerated HJB equations and semilinear parabolic equations. Numerical results are presented in section 4. Some final remarks are given in section 5.

2 Dynamic programming and minimum principle

We consider a filtered complete probability space $(\Omega, \mathcal{F}, \mathbb{F}^B, \mathbb{P})$ with $\mathbb{F}^B := (\mathcal{F}_t)_{0 \leq t \leq T}$ as the natural filtration of the standard q -dimensional Brownian motion $B = (B_t)_{0 \leq t \leq T}$, and $T \in (0, \infty)$ a deterministic terminal time. Let \mathcal{U}_{ad} be the set of admissible feedback control functions defined by

$$\mathcal{U}_{\text{ad}} := \left\{ u : [0, T] \times \mathbb{R}^d \rightarrow U \mid u \text{ is Borel measurable} \right\} \quad \text{with } U \subset \mathbb{R}^m. \quad (3)$$

For any $u \in \mathcal{U}_{\text{ad}}$, the controlled state process X^u is governed by the following stochastic differential equation (SDE):

$$X_t^u = x_0 + \int_0^t \bar{\mu}(s, X_s^u, u(s, X_s^u)) ds + \int_0^t \bar{\sigma}(s, X_s^u, u(s, X_s^u)) dB_s, \quad t \in [0, T], \quad x_0 \in \mathbb{R}^d, \quad (4)$$

where $\bar{\mu} : [0, T] \times \mathbb{R}^d \times U \rightarrow \mathbb{R}^d$ and $\bar{\sigma} : [0, T] \times \mathbb{R}^d \times U \rightarrow \mathbb{R}^d$ are the controlled drift coefficient and controlled diffusion coefficient, respectively, and the stochastic integral with respect to B_s is of Itô type. The cost functional of u is given by

$$J(u) := \mathbb{E} \left[\int_0^T c(s, X_s^u, u(s, X_s^u)) ds + g(X_T^u) \right],$$

where $c : [0, T] \times \mathbb{R}^d \times U \rightarrow \mathbb{R}$ and $g : \mathbb{R}^d \rightarrow \mathbb{R}$ characterize the running cost and terminal cost, respectively. Our main focus is the following SOCP:

$$\text{Find } u^* \in \mathcal{U}_{\text{ad}} \text{ such that } J(u^*) = \inf_{u \in \mathcal{U}_{\text{ad}}} J(u). \quad (5)$$

To carry out the approach of dynamic programming, we define the value function v by

$$v(t, x) = \inf_{u \in \mathcal{U}_{\text{ad}}} J(t, x, u), \quad J(t, x, u) := \mathbb{E} \left[\int_t^T c(s, X_s^u, u(s, X_s^u)) ds + g(X_T^u) \middle| X_t^u = x \right]$$

for $(t, x) \in [0, T] \times \mathbb{R}^d$. Under certain conditions (see, e.g., [43, Theorem 4.3.1 and Remark 4.3.4]), the value function v is the viscosity solution to the following fully nonlinear HJB equation

$$\partial_t v(t, x) + \inf_{\kappa \in U} H(t, x, \kappa, \partial_x v(t, x), \partial_{xx}^2 v(t, x)) = 0, \quad (t, x) \in [0, T] \times \mathbb{R}^d \quad (6)$$

with the terminal condition $v(T, x) = g(x)$, $x \in \mathbb{R}^d$, and the Hamiltonian H given by

$$H(t, x, \kappa, z, p) := \frac{1}{2} \text{Tr} \left(p \bar{\sigma} \bar{\sigma}^\top(t, x, \kappa) \right) + z^\top \bar{\mu}(t, x, \kappa) + c(t, x, \kappa) \quad (7)$$

for $(t, x, \kappa, z, p) \in [0, T] \times \mathbb{R}^d \times U \times \mathbb{R}^d \times \mathbb{R}^{d \times d}$.

Under the regularity condition $v \in C^{1,2}$, i.e., v is once and twice continuously differentiable with respect to $t \in [0, T]$ and $x \in \mathbb{R}^d$, respectively, the classical verification theorem [48, p. 268, Theorem 5.1] reveals the optimal feedback control as

$$u^*(t, X_t^*) \in \arg \min_{\kappa \in U} H(t, X_t^*, \kappa, \partial_x v(t, X_t^*), \partial_{xx}^2 v(t, X_t^*)), \quad t \in [0, T] \quad (8)$$

with $X^* := X^{u^*}$ the controlled diffusion corresponding to the optimal control u^* . The above equation (8) implies that for $t \in [0, T]$

$$H(t, X_t^*, u^*(t, X_t^*), \partial_x v(t, X_t^*), \partial_{xx}^2 v(t, X_t^*)) = \inf_{\kappa \in U} H(t, X_t^*, \kappa, \partial_x v(t, X_t^*), \partial_{xx}^2 v(t, X_t^*)). \quad (9)$$

Therefore, by the minimum principle (9), to find the optimal feedback control, it is

sufficient to ensure

$$u^*(t, x) \in \arg \min_{\kappa \in U} H(t, x, \kappa, \partial_x v(t, x), \partial_{xx}^2 v(t, x)), \quad x \in \Gamma_t, \quad t \in [0, T], \quad (10)$$

or for all $t \in [0, T]$

$$H(t, x, u^*(t, x), \partial_x v(t, x), \partial_{xx}^2 v(t, x)) = \inf_{\kappa \in U} H(t, x, \kappa, \partial_x v(t, x), \partial_{xx}^2 v(t, x)), \quad \forall x \in \Gamma_t \quad (11)$$

for some state set $\Gamma_t \supset \Gamma(X_t^*)$, where $\Gamma(X_t^*)$ denotes the support set of the probability density function of X_t^* .

On the basis of (11), the key step for solving the SCOP (5) is to find the value function v from the HJB equation (6), but, the evaluation of the $\inf_{\kappa \in U} H$ in the the HJB equation (5) and therefore finding $v(t, x)$ suffer from the CoD for a high dimensional control space. However, if the optimal control u^* is known, then from the minimum principle (11), the HJB equation is reduced to, without the inf operation,

$$\partial_t v(t, x) + H(t, x, u^*(t, x), \partial_x v(t, x), \partial_{xx}^2 v(t, x)) = 0, \quad (t, x) \in [0, T] \times \Gamma_t. \quad (12)$$

This argument suggests that we should consider a computational approach, which produces approximations to both the value function $v(t, x)$ and the optimal control u^* , simultaneously, to ensure (12) will hold. This will be the approach discussed in the next section.

3 Proposed method

Throughout this section, we assume the HJB-type equation (1) is non-degenerated, i.e., $\sigma \sigma^\top(t, x)$ is positive definite uniformly for $(t, x) \in [0, T] \times \mathbb{R}^d$. Under the non-degeneracy condition and some usual conditions (see, e.g., [36]), the equation (1) admits a classical solution $v \in C^{1,2}$, where the regularity of v is necessary for our martingale formulation. Nevertheless, the non-degenerated equation (1) is still general enough to cover many useful situations as follows.

- **SOCP (5) without volatility control.** If $\bar{\sigma}(t, x, \kappa) = \bar{\sigma}(t, x)$, the HJB equation (6) degenerates into a special case of (1) with

$$\mathcal{L} = \frac{1}{2} \text{Tr} \left\{ \bar{\sigma} \bar{\sigma}^\top(t, x) \partial_{xx}^2 \right\}, \quad H(t, x, \kappa, z, p) = z^\top \bar{\mu}(t, x, \kappa) + c(t, x, \kappa)$$

for $(t, x, \kappa, z, p) \in [0, T] \times \mathbb{R}^d \times U \times \mathbb{R}^d \times \mathbb{R}^{d \times d}$.

- **Non-degenerated controlled volatility $\bar{\sigma}$ of the SOCP (5).** If the $\bar{\sigma}$ admits a decomposition as $\bar{\sigma}(t, x, \kappa) = \bar{\sigma}_0 I_d + \bar{\sigma}_1(t, x, \kappa)$ with $\bar{\sigma}_0 > 0$, I_q the q -dimensional identity matrix and $\bar{\sigma}_1 \bar{\sigma}_1^\top(t, x, \kappa)$ being positive semidefinite for $(t, x, \kappa) \in [0, T] \times \mathbb{R}^d \times U$, then the HJB equation (6) becomes a special case of (1) with

$$\mathcal{L} = \frac{1}{2} \bar{\sigma}_0^2 \Delta_x, \quad H(t, x, \kappa, z, p) = \frac{1}{2} \text{Tr} \left(p \hat{\sigma}_1 \hat{\sigma}_1^\top(t, x, \kappa) \right) + z^\top \bar{\mu}(t, x, \kappa) + c(t, x, \kappa),$$

for some positive definitive $\hat{\sigma}_1$ (with some conditions imposed on $\bar{\sigma}(t, x, \kappa)$), and $(t, x, \kappa, z, p) \in [0, T] \times \mathbb{R}^d \times U \times \mathbb{R}^d \times \mathbb{R}^{d \times d}$ with $\Delta_x := \text{Tr}(\partial_{xx}^2)$.

- **Knowledge of some preliminary approximation u_0 for the optimal control u^* .** In this case, the HJB equation (6) can be rewritten into (1) with

$$\mathcal{L} = \mathcal{L}^{u_0}, \quad H(t, x, \kappa, \partial_x v(t, x), \partial_{xx}^2 v(t, x)) = (\mathcal{L}^\kappa - \mathcal{L}^{u_0}) v(t, x) + c(t, x, \kappa), \quad (13)$$

where

$$\mathcal{L}^\kappa := \bar{\mu}(t, x, \kappa) \partial_x + \frac{1}{2} \text{Tr} \left\{ \bar{\sigma} \bar{\sigma}^\top (t, x, \kappa) \partial_{xx}^2 \right\} \quad \text{for } \kappa \in U \quad (14)$$

with the convention $\mathcal{L}^u v(t, x) := \mathcal{L}^{u(t, x)} v(t, x)$.

- **Explicit form of the optimal control in the Hamiltonian.** If the following function \bar{H} is explicitly known:

$$\bar{H}(t, x, z, p) := \inf_{u \in U} H(t, x, u, z, p), \quad (t, x, z, p) \in [0, T] \times \mathbb{R}^d \times \mathbb{R}^{d \times d},$$

then (1) degenerates into a special case of semilinear parabolic equations as

$$\partial_t v(t, x) + \mathcal{L}v(t, x) + f(t, x, v(t, x), \partial_x v(t, x), \partial_{xx}^2 v(t, x)) = 0 \quad (15)$$

with f a given function. In (15), f additionally depends on $v(t, x)$ compared with \bar{H} , but this dependence does not pose any difficulties for applying our method to (15); see section 3.4.

From the above discussions, the SOC-MartNet designed for the HJB-type equation (1) is applicable for the SOCP (5) with non-degenerated diffusion and the semilinear parabolic equation (15) without boundary conditions.

3.1 Martingale formulation for HJB-type equations

Let $X : [0, T] \times \Omega \rightarrow \mathbb{R}^d$ be a uncontrolled diffusion process associated with the operator \mathcal{L} , i.e.,

$$X_t = X_0 + \int_0^t \mu(s, X_s) ds + \int_0^t \sigma(s, X_s) dB_s, \quad t \in [0, T]. \quad (16)$$

First, we define two processes - a cost process $\mathcal{M}_t^{u, v}$ and a Hamiltonian process $H_t^{u, v}$ using the optimal control $u \in \mathcal{U}_{\text{ad}}$ and the value function v by

$$\mathcal{M}_t^{u, v} = \mathcal{M}^{u, v}(t, X_t) := v(t, X_t) + \int_0^t H_s^{u, v} ds, \quad (17)$$

$$H_t^{u, v} = H^{u, v}(t, X_t) := H(t, X_t, u(t, X_t), \partial_x v(t, X_t), \partial_{xx}^2 v(t, X_t)), \quad (18)$$

respectively, for $t \in [0, T]$. In the following, we aim at finding a set of sufficient conditions on $\mathcal{M}^{u, v}$ and $H^{u, v}$, under which v will satisfy the HJB-type equation (1), and u is the optimal feedback control in sense of (11), as mentioned in the comment after (12).

Recalling (11), we assume that the uncontrolled diffusion X_t can explore the whole support set of X_t^* (see Remark 1), i.e.,

$$\Gamma(X_t) \supset \Gamma(X_t^*), \quad t \in [0, T]. \quad (19)$$

Then, to establish (11), it is sufficient to consider the condition

$$H_t^{u,v} = H^{u,v}(t, X_t) = \inf_{\kappa \in U} H(t, X_t, \kappa, \partial_x v(t, X_t), \partial_{xx}^2 v(t, X_t)), \quad t \in [0, T]. \quad (20)$$

Remark 1. (State spaces of controlled and uncontrolled diffusion) For the SOCP (5), we introduce the following two strategies to ensure the inclusion condition (19):

- We randomly take the start point X_0 of the uncontrolled diffusion X such that the distribution of X_0 covers a neighborhood of $X_0^* = x_0$ in (4), e.g., $X_0 \sim N(x_0, rI_d)$ with $r > 0$ a hyper parameter.
- The uncontrolled diffusion can be taken as X^{u_0} given by (4) with u_0 an initial approximation of u^* . Then we turn to solve the following equation equivalent to (6):

$$(\partial_t + \mathcal{L}^{u_0})v(t, x) + \inf_{\kappa \in U} \{(\mathcal{L}^\kappa - \mathcal{L}^{u_0})v(t, x) + c(t, x, \kappa)\} = 0, \quad (t, x) \in [0, T] \times \mathbb{R}^d,$$

for which the Hamiltonian process in (18) is given by

$$H_t^{u,v} = (\mathcal{L}^u - \mathcal{L}^{u_0})v(t, X_t^{u_0}) + c(t, X_t^{u_0}, u(t, X_t^{u_0})), \quad t \in [0, T].$$

The condition (20) is computationally intractable because minimizing the Hamiltonian H for each time-state (t, X_t) is too expensive, resulting in a CoD problem. To avoid this issue, we introduce the following lemma.

Lemma 1. Let u be any function in \mathcal{U}_{ad} and $v : [0, T] \times \mathbb{R}^d \rightarrow \mathbb{R}$ be any function satisfying $\int_0^T \mathbb{E} [|H_t^{u,v}|] dt < +\infty$. Then

$$H_t^{u,v} = \inf_{\kappa \in U} H(t, X_t, \kappa, \partial_x v(t, X_t), \partial_{xx}^2 v(t, X_t)), \quad \forall (t, \omega) \in [0, T] \times \Omega, \text{ a.e. } -dt \times \mathbb{P}, \quad (21)$$

if and only if

$$\int_0^T \mathbb{E} [H_t^{u,v}] dt = \inf_{\bar{u} \in \mathcal{U}_{\text{ad}}} \int_0^T \mathbb{E} [H_t^{\bar{u},v}] dt. \quad (22)$$

Proof. (21) \Rightarrow (22): It follows from (3) trivially.

(22) \Rightarrow (21): By (3) and the definition of infimum, for any $\delta > 0$, there exists $u_\delta \in \mathcal{U}_{\text{ad}}$ such that the following inequality between two functions of two variables (t, X_t) hold, i.e.,

$$H_t^{u_\delta, v} = H^{u_\delta, v}(t, X_t) < \inf_{\kappa \in U} H(t, X_t, \kappa, \partial_x v(t, X_t), \partial_{xx}^2 v(t, X_t)) + \delta \text{ for } t \in [0, T],$$

where $H_t^{u_\delta, v} = H^{u_\delta, v}(t, X_t)$ is given in (18). Then taking $\int_0^T \mathbb{E} [\cdot] dt$ on both sides of the above inequality, we have that

$$\int_0^T \mathbb{E} [H_t^{u_\delta, v}] dt \leq \int_0^T \mathbb{E} \left[\inf_{\kappa \in U} H(t, X_t, \kappa, \partial_x v(t, X_t), \partial_{xx}^2 v(t, X_t)) \right] dt + \delta T.$$

Combining the above equality and (22), we have that

$$\int_0^T \mathbb{E} [H_t^{u,v}] dt \leq \int_0^T \mathbb{E} \left[\inf_{\kappa \in U} H(t, X_t, \kappa, \partial_x v(t, X_t), \partial_{xx}^2 v(t, X_t)) \right] dt + \delta T,$$

i.e.,

$$\int_0^T \mathbb{E}[\varepsilon_t] dt \leq \delta T \quad \text{with} \quad \varepsilon_t = \varepsilon(t, X_t) := H_t^{u,v} - \inf_{\kappa \in U} H(t, X_t, \kappa, \partial_x v(t, X_t), \partial_{xx}^2 v(t, X_t)). \quad (23)$$

Since $\delta > 0$ is arbitrary, the above inequality implies $\int_0^T \mathbb{E}[\varepsilon_t] dt \leq 0$. On the other hand, the definition of $\varepsilon(t, X_t)$ implies that ε_t is a nonnegative function of (t, X_t) , namely, $\varepsilon_t \geq 0$ for any $t \in [0, T]$, and thus we obtain

$$\varepsilon_t = 0 \quad \text{for} \quad (t, \omega) \in [0, T] \times \Omega, \quad \text{a.e.-} dt \times \mathbb{P},$$

which is just (21). □

Remark 2. (Independent sampling in (t, x) variables) Compared to (21), the equivalent condition (22) offers significant computational benefits, as the minimization is imposed on a single functional of the control space instead of the Hamiltonian over time-state (t, X_t) space in addition to the control space. Moreover, the double integral introduced here in practice is only carried over a cone shape region in the space-time domain, and this condition will allow independent sampling of t and x to be carried out for computation speed-up from parallel efficiency.

Utilizing the condition (21), we can simplify the HJB-type equation (1) into

$$(\partial_t + \mathcal{L})v(t, X_t) = -H_t^{u,v}(t, X_t) \quad (24)$$

for $t \in [0, T]$. Next, we will show that (24) can be fulfilled by enforcing the cost process $\mathcal{M}^{u,v}$ in (17) to be a martingale with the value function v and the optimal control u . The following lemma presents the details.

Lemma 2. For any $(u, v) \in \mathcal{U}_{\text{ad}} \times C^{1,2}$ satisfying

$$\int_0^T \mathbb{E} \left[|\partial_x v \sigma(t, X_t)|^2 \right] dt < \infty, \quad \int_0^T \mathbb{E} \left[|H_t^{u,v}|^2 \right] dt < \infty, \quad \mathbb{E} \left[|v(T, X_T)|^2 \right] < \infty, \quad (25)$$

the equation (24) holds for $(t, \omega) \in [0, T] \times \Omega$ a.e.- $dt \times \mathbb{P}$ if and only if $M_t^{u,v}(t, X_t)$ is a \mathbb{F}^B -martingale, i.e.,

$$\mathcal{M}_t^{u,v} = \mathbb{E} \left[\mathcal{M}_T^{u,v} | \mathcal{F}_t \right], \quad t \in [0, T]. \quad (26)$$

Proof. For $v \in C^{1,2}$, the Itô's formula implies that

$$v(t, X_t) = v(0, X_0) + \int_0^t (\partial_t + \mathcal{L})v(s, X_s) ds + \int_0^t \partial_x v \sigma(s, X_s) dB_s, \quad t \in [0, T]. \quad (27)$$

(24) \Rightarrow (26): Inserting (24) into the above equation and further using the definition of (17), we obtain

$$\mathcal{M}_t^{u,v} = v(t, X_t) + \int_0^t H^{u,v}(s, X_s) ds = v(0, X_0) + \int_0^t \partial_x v \sigma(s, X_s) dB_s, \quad t \in [0, T],$$

Then $M_t^{u,v}(t, X_t)$ is a martingale from the above equation combined with the first condition in (25), thus (26) holds.

(26) \Rightarrow (24): Recalling again the definition in (17), the last two conditions in (25) implies that $\mathbb{E}[|\mathcal{M}_T^{u,v}|^2] < \infty$. Then by the martingale representation theorem [41, Theorem 4.3.4], there exists a square integrable and \mathbb{F}^B -adapted process $Z : [0, T] \times \Omega \rightarrow \mathbb{R}^q$ such that

$$\mathcal{M}_t^{u,v} = \mathcal{M}_0^{u,v} + \int_0^t Z_s dB_s, \quad t \in [0, T].$$

By using the definition $\mathcal{M}_t^{u,v}$ in (17) above, we then have

$$v(t, X_t) = v(0, X_0) - \int_0^t H^{u,v}(s, X_s) ds + \int_0^t Z_s dB_s. \quad (28)$$

Combining (27) and (28), we have that

$$Q_t := \int_0^t \{(\partial_t + \mathcal{L})v(s, X_s) + H^{u,v}(s, X_s)\} ds = \int_0^t \{\partial_x v \sigma(s, X_s) - Z_s\} dB_s, \quad t \in [0, T].$$

which means that Q is a finite variation process, and is also a continuous martingale. Thus it follows from [18, Theorem 4.8] that $Q_t = 0$ for $t \in [0, T]$, a.s., which validates (24). \square

Lemmas 1 and 2 directly lead to the following theorem, which presents our martingale formulation (29) for the HJB-type equation (1).

Theorem 3. *Assume $(u, v) \in \mathcal{U}_{\text{ad}} \times C^{1,2}$ satisfies (25). Let $M_t^{u,v}$ and $H_t^{u,v}$ be given by (17) and (18), respectively. Then the following two conditions*

$$\int_0^T \mathbb{E}[H_t^{u,v}] dt = \inf_{\bar{u} \in \mathcal{U}_{\text{ad}}} \int_0^T \mathbb{E}[H_t^{\bar{u},v}] dt, \quad \mathcal{M}_t^{u,v} = \mathbb{E}[\mathcal{M}_T^{u,v} | \mathcal{F}_t], \quad t \in [0, T], \quad (29)$$

are equivalent to

$$(\partial_t + \mathcal{L})v(t, X_t) = - \inf_{\kappa \in U} H(t, X_t, \kappa, \partial_x v(t, X_t), \partial_{xx}^2 v(t, X_t)) \quad (30)$$

for $(t, \omega) \in [0, T] \times \Omega$, a.e.- $dt \times \mathbb{P}$.

Now based on Theorem 3, the key issue is to fulfill the minimum condition and the martingale condition in (29), to be achieved by the SOC-MartNet algorithm.

3.2 SOC-MartNet via adversarial learning for control/value functions

To avoid computing conditional expectations as in the original DeepMartNet [7; 8], we modify the martingale condition in (29) into

$$\sup_{\rho \in \mathcal{T}} \left| \int_0^{T-\Delta t} \mathbb{E}[\rho(t, X_t) (\mathcal{M}_{t+\Delta t}^{u,v} - \mathcal{M}_t^{u,v})] dt \right|^2 = 0, \quad (31)$$

where \mathcal{T} denotes the set of test functions, defined by

$$\mathcal{T} := \left\{ \rho : [0, T] \times \mathbb{R}^d \rightarrow \mathbb{R} \mid \rho \text{ is smooth and bounded} \right\}, \quad (32)$$

and $\Delta t \in (0, T)$ is the time step size. For sufficiently small Δt , condition (31) ensures the martingale condition in (29). Actually, by the property of conditional expectations,

it holds that

$$\mathbb{E} [\rho(t, X_t)(\mathcal{M}_{t+\Delta t}^{u,v} - \mathcal{M}_t^{u,v})] = \mathbb{E} [\rho(t, X_t)\mathbb{E} [(\mathcal{M}_{t+\Delta t}^{u,v} - \mathcal{M}_t^{u,v})|X_t]], \quad t \in [0, T - \Delta t]. \quad (33)$$

Inserting (33) into (31), we have that

$$\int_0^{T-\Delta t} \mathbb{E} [\rho(t, X_t)\mathbb{E} [(\mathcal{M}_{t+\Delta t}^{u,v} - \mathcal{M}_t^{u,v})|X_t]] dt = 0 \quad \text{for all } \rho \in \mathcal{T},$$

where $\mathbb{E} [(\mathcal{M}_{t+\Delta t}^{u,v} - \mathcal{M}_t^{u,v})|X_t]$ is a deterministic and Borel measurable function of (t, X_t) [34, Corollary 1.97], and thus,

$$\mathbb{E} [(\mathcal{M}_{t+\Delta t}^{u,v} - \mathcal{M}_t^{u,v})|X_t] = 0, \quad (t, \omega) \in [0, T - \Delta t] \times \Omega, \quad \text{a.e.-} dt \times \mathbb{P}. \quad (34)$$

The above conditions implies that $\mathcal{M}^{u,v}$ satisfies the martingale condition in (29) approximately for sufficiently small Δt .

A unique feature of (31) lies in its natural connection to adversarial learning [49], based on which, we can fulfill the conditions (2) and (29) by

$$(u, v) = \lim_{\lambda \rightarrow +\infty} \arg \min_{(\bar{u}, \bar{v}) \in \mathcal{U}_{\text{ad}} \times \mathcal{V}} \left\{ \sup_{\rho \in \mathcal{T}} \mathbb{L}(\bar{u}, \bar{v}, \rho, \lambda) \right\} \quad (35)$$

where \mathcal{U}_{ad} is given in (3), and \mathcal{V} is the set of candidate value functions satisfying (2), i.e.,

$$\mathcal{V} := \left\{ v : [0, T] \times \mathbb{R}^d \rightarrow \mathbb{R} \mid v \in C^{1,2}, v(T, x) = g(x), \forall x \in \mathbb{R}^d \right\}, \quad (36)$$

and \mathbb{L} is the augmented Lagrangian defined by

$$\mathbb{L}(u, v, \rho, \lambda) := \int_0^T \mathbb{E} [H_t^{u,v}] dt + \lambda \left| \int_0^{T-\Delta t} \mathbb{E} [\rho(t, X_t) (\mathcal{M}_{t+\Delta t}^{u,v} - \mathcal{M}_t^{u,v})] dt \right|^2 \quad (37)$$

with λ the multiplier being sufficiently large.

For adversarial learning, we replace the functions u , v and ρ by the control network $u_\alpha : [0, T] \times \mathbb{R}^d \rightarrow U$, the value network $v_\theta : [0, T] \times \mathbb{R}^d \rightarrow \mathbb{R}$ and the adversarial network $\rho_\eta : [0, T] \times \mathbb{R}^d \rightarrow \mathbb{R}^r$ parameterized by α , θ and η , respectively. Since the range of u_α should be restricted in the control space U , if $U = [a, b] := \prod_{i=1}^m [a_i, b_i]$ with a_i, b_i the i -th elements of $a, b \in \mathbb{R}^m$, the structure of u_α can be

$$u_\alpha(t, x) = a + \frac{b-a}{6} \text{ReLU6}(\psi_\alpha(t, x)), \quad (t, x) \in [0, T] \times \mathbb{R}^d, \quad (38)$$

where $\text{ReLU6}(y) := \min\{\max\{0, y\}, 6\}$ is an activation function and $\psi_\alpha : [0, T] \times \mathbb{R}^d \rightarrow \mathbb{R}^m$ is a neural network with parameter α . Remark 3 provides a penalty method to deal with general control spaces. To satisfy the terminal condition in (36), the value network v_θ takes the form of

$$v_\theta(t, x) = \begin{cases} \phi_\theta(t, x), & 0 \leq t < T, \\ g(x), & t = T \end{cases} \quad (39)$$

with $\phi_\theta : [0, T] \times \mathbb{R}^d \rightarrow \mathbb{R}$ a neural network parameterized by θ . The adversarial network ρ_η plays the role of test functions. By our experiment results, ρ_η is not necessarily to be very deep, but instead, it can be a shallow network with enough output dimensionality.

A typical example is that

$$\rho_\eta(t, x) = \sin(W_1 t + W_2 x + b) \in \mathbb{R}^r, \quad \eta := (W_1, W_2, b) \in \mathbb{R}^r \times \mathbb{R}^{r \times d} \times \mathbb{R}^r \quad (40)$$

for $(t, x) \in [0, T] \times \mathbb{R}^d$, where $\sin(\cdot)$ is the activation function applied on $W_1 t + W_2 x + b$ in an element-wise manner.

SOC-MartNet Based on (35) and (37) with $(u_\alpha, v_\theta, \rho_\eta)$ in place of (u, v, ρ) , the solution (u, v) of (35) can be approximated by $(u_{\alpha^*}, v_{\theta^*})$ given by

$$(\alpha^*, \theta^*) = \lim_{\lambda \rightarrow +\infty} \arg \min_{\alpha, \theta} \left\{ \max_{\eta} L(\alpha, \theta, \eta, \lambda) \right\}, \quad (41)$$

where

$$L(\alpha, \theta, \eta, \lambda) := \int_0^T \mathbb{E}[H_t^{u_\alpha, v_\theta}] dt + \lambda \left| \int_0^{T-\Delta t} \mathbb{E}[\rho_\eta(t, X_t) (\mathcal{M}_{t+\Delta t}^{u_\alpha, v_\theta} - \mathcal{M}_t^{u_\alpha, v_\theta})] dt \right|^2 \quad (42)$$

with H^{u_α, v_θ} and M^{u_α, v_θ} given in (17) and (18), respectively. The proposed method will be named SOC-MartNet for SOCPs as it is based on the martingale condition of the cost process (26), similar to the DeepMartNet [7; 8].

Remark 3. *If the control space U is general rather than an interval, the network structure in (38) is no longer applicable. This issue can be addressed by appending a new penalty term on the right side of (42) to ensure $u_\alpha(t, X_t)$ remains within U . The following new loss function is an example:*

$$\bar{L}(\alpha, \theta, \eta, \lambda, \bar{\lambda}) := L(\alpha, \theta, \eta, \lambda) + \bar{\lambda} \int_0^T \mathbb{E}[\text{dist}(u_\alpha(t, X_t), U)] dt,$$

where $L(\alpha, \theta, \eta, \lambda)$ is given in (42); $\bar{\lambda} \geq 0$ is a multiplier and $\text{dist}(\kappa, U)$ denotes a certain distance between $\kappa \in \mathbb{R}^m$ and U .

3.3 Training algorithm

To solve (41) numerically, we introduce a time partition on the time interval $[0, T]$, i.e.,

$$\pi_N := \{t_0, t_1, \dots, t_N\} \text{ s.t. } 0 = t_0 < t_1 < t_2 < \dots < t_n < t_{n+1} < \dots < t_N = T. \quad (43)$$

For $n = 0, 1, \dots, N-1$, denote

$$\Delta t_n := t_{n+1} - t_n, \quad \Delta B_{n+1} := B_{n+1} - B_n.$$

Then we apply the following numerical approximations on the loss function in (42):

1. The process $(X_{t_n})_{n=0}^N$ can be approximated by $(X_n)_{n=0}^N$, which is obtained by applying the Euler scheme to the SDE (16), i.e.,

$$X_{n+1} = X_n + \mu(t_n, X_n)\Delta t_n + \sigma(t_n, X_n)\Delta B_{n+1}, \quad n = 0, 1, 2, \dots, N-1. \quad (44)$$

2. The integral in (17) can be approximated by the trapezoid formula, resulting that

$\mathcal{M}_{t_{n+1}}^{u_\alpha, v_\theta} - \mathcal{M}_{t_n}^{u_\alpha, v_\theta} \approx \Delta \mathcal{M}_{n+1}^{\alpha, \theta}$ with

$$\Delta \mathcal{M}_{n+1}^{\alpha, \theta} := v_\theta(t_{n+1}, X_{n+1}) - v_\theta(t_n, X_n) - \frac{1}{2} \left(H_n^{\alpha, \theta} + H_{n+1}^{\alpha, \theta} \right) \Delta t_n, \quad (45)$$

and

$$H_n^{\alpha, \theta} := H(t_n, X_n, u_\alpha(t_n, X_n), \partial_x v_\theta(t_n, X_n), \partial_{xx}^2 v_\theta(t_n, X_n)), \quad n = 0, 1, \dots, N. \quad (46)$$

3. The expectations in (42) can be approximated by the Monte-Carlo method based on the i.i.d. samples of $\{(X_n, H_n^{\alpha, \theta}, \Delta \mathcal{M}_n^{\alpha, \theta})\}_{n=0}^N$, i.e.,

$$\{(X_n^{(m)}, H_n^{\alpha, \theta, (m)}, \Delta \mathcal{M}_n^{\alpha, \theta, (m)})\}_{n=0}^N, \quad m = 1, 2, \dots, M. \quad (47)$$

Combining the above approximations, the loss function in (42) is replaced by its mini-batch version as

$$L(\alpha, \theta, \eta, \lambda; A) := \frac{1}{|A|} \sum_{(n, m) \in A} H_n^{\alpha, \theta, (m)} \Delta t_n + \lambda |G(\alpha, \theta, \eta, \lambda; A)|^2, \quad (48)$$

$$G(\alpha, \theta, \eta; A) := \frac{1}{|A|} \sum_{(n, m) \in A} \rho_\eta(t_n, X_n^{(m)}) \Delta \mathcal{M}_{n+1}^{\alpha, \theta, (m)} \Delta t_n \quad (49)$$

with $\Delta t_N := \Delta \mathcal{M}_{N+1}^{\alpha, \theta} := 0$ for convenience, where A is a index subset randomly taken from $\{0, 1, \dots, N\} \times \{1, 2, \dots, M\}$ and is updated at each optimization step. The loss function in (48) can be optimized by alternating gradient descent and ascent of $L(\alpha, \theta, \eta, \lambda; A)$ over (α, θ) and (λ, η) , respectively. The details are presented in Algorithm 1.

Remark 4. *In our martingale formulation, the diffusion process X given by (16) is fixed and independent of the control and the value function, and thus its sample paths can be generated offline before optimizing the loss function in (48). Moreover, in the SOC-MartNet, the gradient computation for the loss function and the training of neural networks are both free of recursive iterations along the time direction, which contributes to significant efficiency gains for the SOC-MartNet. This feature is different from many existing deep-learning probabilistic methods for PDEs, e.g., [1; 14; 24; 25; 28; 39; 50; 52]. Our numerical experiments in section 4 confirm the high efficiency of the SOC-MartNet.*

3.4 Application to parabolic problems

The SOC-MartNet proposed in the last subsection is applicable for the HJB-type equation (1). In this section, we explore how SOC-MartNet can be tailored to the parabolic equation (15), yielding enhanced efficiency and simplicity.

Specifically, by (17) with f in place of H , we obtain a new cost process $\tilde{\mathcal{M}}^v$ independent of u , i.e.,

$$\tilde{\mathcal{M}}_t^v := v(t, X_t) + \int_0^t f(s, X_s, v(t, X_t), \partial_x v(t, X_t), \partial_{xx}^2 v(t, X_t)) ds, \quad t \in [0, T].$$

Algorithm 1 SOC-MartNet for solving the HJB-type equation (1)

Input: I : the maximum number of iterations; M : the total number of sample paths of diffusion process from (44); $\delta_1/\delta_2/\delta_3/\delta_4$: learning rates for control network u_α /value network v_θ /adversarial network ρ_η /multiplier λ ; J/K : number of $(\alpha, \theta)/(\lambda, \eta)$ updates per iteration.

- 1: Initialize the networks $u_\alpha, v_\theta, \rho_\eta$ and the multiplier λ
- 2: Generate the sample paths $\{X_n^{(m)}\}_{n=0}^N$ for $m = 1, 2, \dots, M$ by (44)
- 3: **for** $i = 0, 1, \dots, I - 1$ **do**
- 4: Sample the index subset $A_i \subset \{0, 1, \dots, N - 1\} \times \{1, 2, \dots, M\}$ per (54)
- 5: **for** $j = 0, 1, \dots, J - 1$ **do**
- 6: $\alpha \leftarrow \alpha - \delta_1 \nabla_\alpha L(\alpha, \theta, \eta, \lambda; A_i)$ // L is computed by (48)
- 7: $\theta \leftarrow \theta - \delta_2 \nabla_\theta L(\alpha, \theta, \eta, \lambda; A_i)$
- 8: **end for**
- 9: **for** $k = 0, 1, \dots, K - 1$ **do**
- 10: $\eta \leftarrow \eta + \delta_3 \nabla_\eta L(\alpha, \theta, \eta, \lambda; A_i)$
- 11: $\lambda \leftarrow \lambda + \delta_4 |G(\alpha, \theta, \eta; A_i)|^2$ // G is computed by (49)
- 12: **end for**
- 13: **end for**

Output: u_α and v_θ

Under some regularity conditions, by following the deductions in section 3.1, we conclude that v satisfies the equation (1) in sense of (30) if and only if $\tilde{\mathcal{M}}^v$ is a \mathbb{F}^B -martingale. Thus the value function v_{θ^*} can be learned through adversarial training to enforce the martingale property of $\tilde{\mathcal{M}}^v$, i.e.,

$$\theta^* = \arg \min_{\theta} \left\{ \max_{\eta} \tilde{G}(\theta, \eta) \right\}, \quad \tilde{G}(\theta, \eta) := \left| \int_0^{T-\Delta t} \mathbb{E} \left[\rho_\eta(t, X_t) \left(\tilde{\mathcal{M}}_{t+\Delta t}^{v_\theta} - \tilde{\mathcal{M}}_t^{v_\theta} \right) \right] dt \right|^2. \quad (50)$$

To learn the value function from (50), at each iteration step, the loss function $\tilde{G}(\theta, \eta)$ is replaced by its mini-batch version defined as

$$\tilde{G}(\theta, \eta; A) := \frac{1}{|A|} \sum_{(n,m) \in A} \rho_\eta(t_n, X_n^{(m)}) \Delta \tilde{\mathcal{M}}_{n+1}^{\theta, (m)} \Delta t_n, \quad (51)$$

where A is a index subset randomly taken from $\{0, 1, \dots, N\} \times \{1, 2, \dots, M\}$ and

$$\begin{aligned} \Delta \tilde{\mathcal{M}}_{n+1}^{\theta, (m)} &:= v_\theta(t_{n+1}, X_{n+1}^{(m)}) - v_\theta(t_n, X_n^{(m)}) - \frac{1}{2} \left(f_n^{\theta, (m)} + f_{n+1}^{\theta, (m)} \right) \Delta t_n, \\ f_n^{\theta, (m)} &:= f \left(t_n, X_n^{(m)}, v_\theta(t_n, X_n^{(m)}), \partial_x v_\theta(t_n, X_n^{(m)}), \partial_{xx}^2 v_\theta(t_n, X_n^{(m)}) \right), \end{aligned}$$

and $X_n^{(m)}$ is introduced in (47). Algorithm 2 presents the detailed procedures of the SOC-MartNet for parabolic equations.

4 Numerical tests

As a benchmark, we consider the method of FBSNN proposed in [50, Scheme 2]. We briefly review the FBSNN for the parabolic equation (15). To approximate v , let $v_\theta : [0, T] \times \mathbb{R}^d \rightarrow \mathbb{R}$ be a neural network in form of (39), where the terminal condition

Algorithm 2 SOC-MartNet for solving the parabolic equation (15)

Input: I : the maximum number of iterations; M : the total number of sample paths of diffusion process from (44); δ_2/δ_3 : learning rates for value network v_θ /adversarial network ρ_η ; J/K : number of θ/η updates per iteration.

- 1: Initialize the networks v_θ and ρ_η
- 2: Generate the sample paths $\{X_n^{(m)}\}_{n=0}^N$ for $m = 1, 2, \dots, M$ by (44)
- 3: **for** $i = 0, 1, \dots, I - 1$ **do**
- 4: Sample the index subset $A_i \subset \{0, 1, \dots, N - 1\} \times \{1, 2, \dots, M\}$ per (54)
- 5: **for** $j = 0, 1, \dots, J - 1$ **do**
- 6: $\theta \leftarrow \theta - \delta_2 \nabla_\theta \tilde{G}(\theta, \eta; A_i)$ // \tilde{G} is computed by (51)
- 7: **end for**
- 8: **for** $k = 0, 1, \dots, K - 1$ **do**
- 9: $\eta \leftarrow \eta + \delta_3 \nabla_\eta \tilde{G}(\theta, \eta; A_i)$
- 10: **end for**
- 11: **end for**

Output: v_θ

of (15) has been encoded into the definition of v_θ . Then the loss function of FBSNN is that

$$L_{\text{fbsnn}}(\theta) := \frac{1}{N} \frac{1}{|A|} \sum_{n=1}^N \sum_{m \in A} \left| v_\theta(t_n, X_n^{(m)}) - \tilde{v}_{\theta,n}^{(m)} \right|^2, \quad (52)$$

where A is a index subset of $\{1, 2, \dots, M\}$, and $\tilde{v}_{\theta,n}^{(m)}$ is given by

$$\begin{aligned} \tilde{v}_{\theta,n}^{(m)} &= \tilde{v}_{\theta,n-1}^{(m)} - f\left(t_{n-1}, X_{n-1}^{(m)}, \tilde{v}_{\theta,n-1}^{(m)}, \partial_x v_\theta(t_{n-1}, X_{n-1}^{(m)}), \partial_{xx}^2 v_\theta(t_{n-1}, X_{n-1}^{(m)})\right) \Delta t_{n-1} \\ &\quad + \partial_x v_\theta(t_{n-1}, X_{n-1}^{(m)}) \Delta B_n^{(m)} \end{aligned}$$

with $\tilde{v}_{\theta,0}^{(m)} := v_\theta(t_0, X_0^{(m)})$.

In the tests, all the involved methods solve $v(0, x)$ for $x \in S_1 \cup S_2$, where S_1 and S_2 are two spatial line segments defined by

$$S_i := \{s e_i : s \in [-1, 1]\} \quad \text{for } e_1 := (1, 0, 0, \dots, 0)^\top \in \mathbb{R}^d, \quad e_2 := (1, 1, \dots, 1)^\top \in \mathbb{R}^d.$$

For an approximation \hat{v} of v , its relative error $R(\hat{v})$ is given by

$$R(\hat{v}) := \frac{\sum_{x \in D_0} |\hat{v}(0, x) - v(0, x)|}{\sum_{x \in D_0} |v(0, x)|},$$

where D_0 consists of M uniformly-spaced grid points on the two line segments S_1 and S_2 , i.e.,

$$D_0 = \bigcup_{i=1,2} \bigcup_{j=0}^{M-1} \left\{ \left(\frac{2j}{K-1} - 1 \right) e_i \right\}. \quad (53)$$

If no otherwise specified, we take $T = 1$ and $N = 100$ for all involved loss functions, and all the loss functions are minimized by the RMSProp algorithm. Each point in D_0 are selected as the start point $X_0^{(m)}$ of the sample paths in (44), i.e., $\{X_0^{(m)} : m = 0, 1, \dots, M\} = D_0$, where the total number M of sample paths is set to 10^5 for $d \leq 500$ and 10^4 for $d > 500$.

Sampling of index set A_i . For the SOC-MartNet given by Algorithm 1 and Algorithm 2, the index subset A_i on Line 4 is taken as

$$A_i = \{0, 1, 2, \dots, N\} \times M_i, \quad (54)$$

where M_i is a random subset of $\{1, 2, \dots, M\}$ with its size $|M_i| = 200, 400, 800, 1600$ for $i \leq 0.25I$, $0.25I < i \leq 0.5I$, $0.5I < i \leq 0.75I$ and $0.75I < i \leq I$, respectively. The number I of iteration steps are set to 10^3 for $d \leq 500$ and 2×10^3 for $d > 500$. The learning rates on Lines 6, 7 and 10 of Algorithm 1 are set to

$$\delta_1 = \delta_2 = \delta_0 \times 0.01^{i/I}, \quad \delta_3 = 10^{-2} \times 0.01^{i/I}, \quad i = 0, 1, \dots, I-1 \quad (55)$$

with $\delta_0 = 10^{-3}$ for $d \leq 100$ and $\delta_0 = 10^{-4}$ for $d > 100$. The initial value of λ is 10 with its learning rate $\delta_4 = 10$ and its upper bound set to 10^4 . The inner iteration steps are $J = 2K = 2$. The neural networks u_α and v_θ both consist of 4 hidden layers with $2d + 20$ ReLU units in each hidden layer. The adversarial network ρ_η is given by (40) with the output dimensionality $r = 2d + 300$.

For FBSNN given by (52), the learning rate in the i -th iteration step is $10^{-3 \times (1+i/I)}$; the batch size $|A|$ is taken as 300 and other parameter settings are the same as the ones of SOC-MartNet.

All the tests are implemented by Python 3.12 and PyTorch 2.2. If no otherwise specified, the algorithm is accelerated by the strategy of Distributed Data Parallel (DDP)¹ on a compute node equipped with 8 GPUs (NVIDIA Tesla V100-SXM2-32GB). When reporting the numerical results, “RE”, “vs” and “Hamilt.” are short for “Relative error”, “versus” and “Hamiltonian”, respectively, where $\text{Hamilt.} := 1/|A| \sum_{(n,m) \in A} H_n^{\alpha, \theta, (m)} \Delta t_n$ recalling (48). The term “Mart. Loss” denotes the value of $G(\alpha, \theta, \eta; A)$ defined in (49).

4.1 Linear parabolic problem

We consider the following problem:

$$\begin{cases} (\partial_t + \frac{1}{2}\Delta_x)v(t, x) - f(t, x) = 0, & (t, x) \in [0, T] \times \mathbb{R}^d, \\ v(T, x) = g(x), & x \in \mathbb{R}^d, \end{cases} \quad (56)$$

where f and g are chosen such that v is given by

$$v(t, x) = 1 + \frac{1}{d} \sum_{i=1}^d \sin(t + x_i), \quad (t, x) \in [0, T] \times \mathbb{R}^d. \quad (57)$$

Figures 1 to 5 show the numerical results of SOC-MartNet (Algorithm 2) and FBSNN for solving the parabolic problem (56) with $d = 50, 100, 500, 1000$. The numerical results demonstrate that the SOC-MartNet is effective for problems with dimensionality upto 1000. By Figure 5, it seems that SOC-MartNet’s advantage becomes more significant as the dimensionality increases.

¹https://github.com/pytorch/tutorials/blob/main/intermediate_source/ddp_tutorial.rst

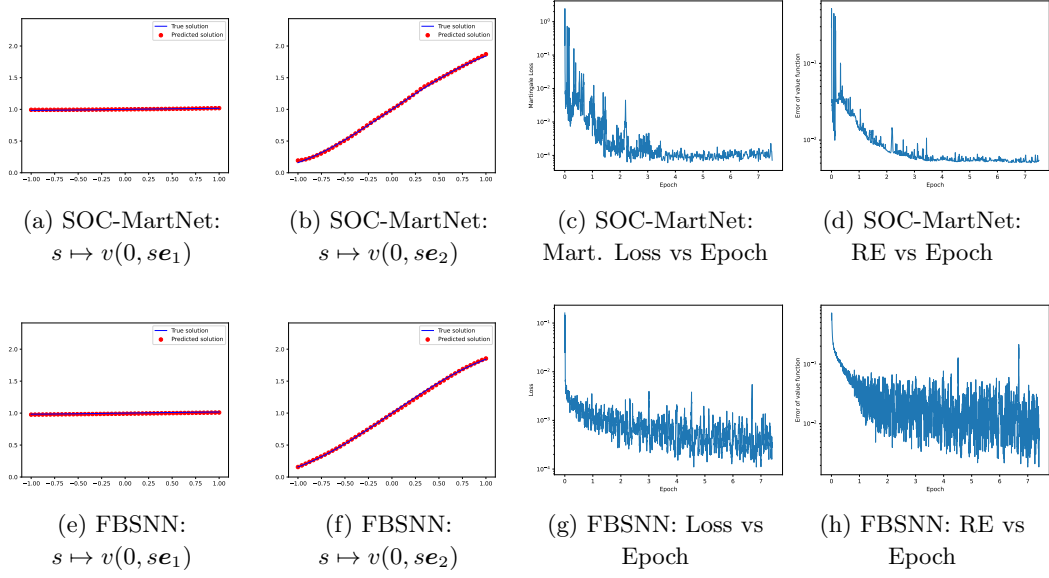


Figure 1: Numerical results for the linear parabolic problem (56) with $d = 50$. The running times of SOC-MartNet and FBSNN are 14 and 105 seconds, respectively.

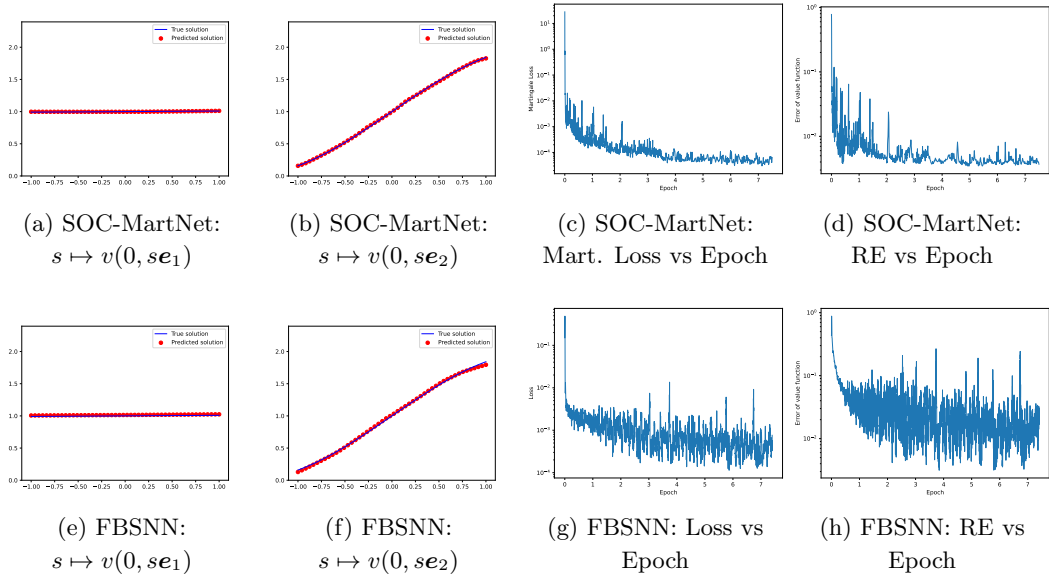


Figure 2: Numerical results for the linear parabolic problem (56) with $d = 100$. The running times of SOC-MartNet and FBSNN are 18 and 105 seconds, respectively.

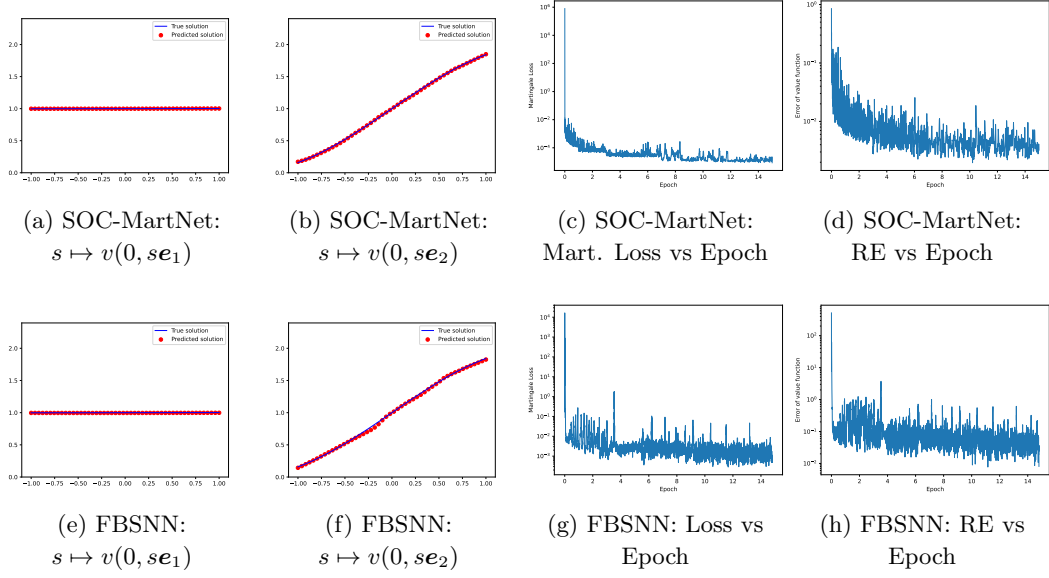


Figure 3: Numerical results for the linear parabolic problem (56) with $d = 500$. The running times of SOC-MartNet and FBSNN are 203 and 309 seconds, respectively.

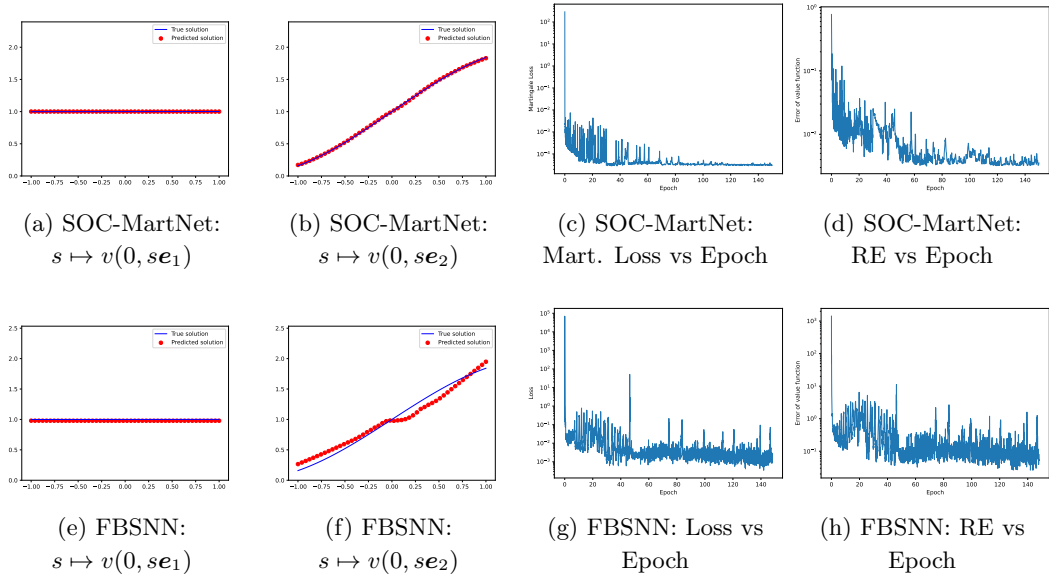


Figure 4: Numerical results for the linear parabolic problem (56) with $d = 1000$. The running times of SOC-MartNet and FBSNN are 401 and 494 seconds, respectively.

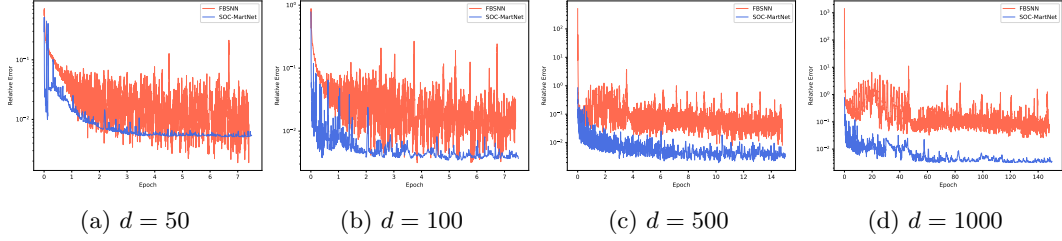


Figure 5: The RE vs Epoch for SOC-MartNet and FBSNN in solving the linear parabolic problem (56).

4.2 Semilinear parabolic equation

We consider the following parabolic equation from [14, Section 4.3]:

$$\begin{cases} (\partial_t + \Delta_x) v(t, x) - |\partial_x v(t, x)|^2 = 0, & (t, x) \in [0, T] \times \mathbb{R}^d, \\ v(T, x) = 1 + g(x), & x \in \mathbb{R}^d, \end{cases} \quad (58)$$

where the function $g : \mathbb{R}^d \rightarrow \mathbb{R}$ will be specified later. The problem (58) admits an analytic solution as

$$v(t, x) = 1 - \ln \left(\mathbb{E} \left[\exp \left(-g(x + \sqrt{2}B_{T-t}) \right) \right] \right), \quad (t, x) \in [0, T] \times \mathbb{R}^d. \quad (59)$$

To compute the absolute error of numerical solutions, the analytic solution in (59) is approximated by the Monte-Carlo method applied on the expectation using 10^6 i.i.d. samples of B_{T-t} .

4.2.1 Smooth terminal function

In the following, we consider (58) with a terminal function as

$$g(x) := \ln \left(\frac{1}{2}(1 + |x|^2) \right). \quad (60)$$

This example is also considered by [1; 14]. We test the SOC-MartNet (Algorithm 2) and FBSNN for $d = 50, 100, 500, 1000$. The relevant numerical results are presented in Figures 6 to 10, where the SOC-MartNet behaves well and enjoys a significant advantage for $d = 500$ and 1000.

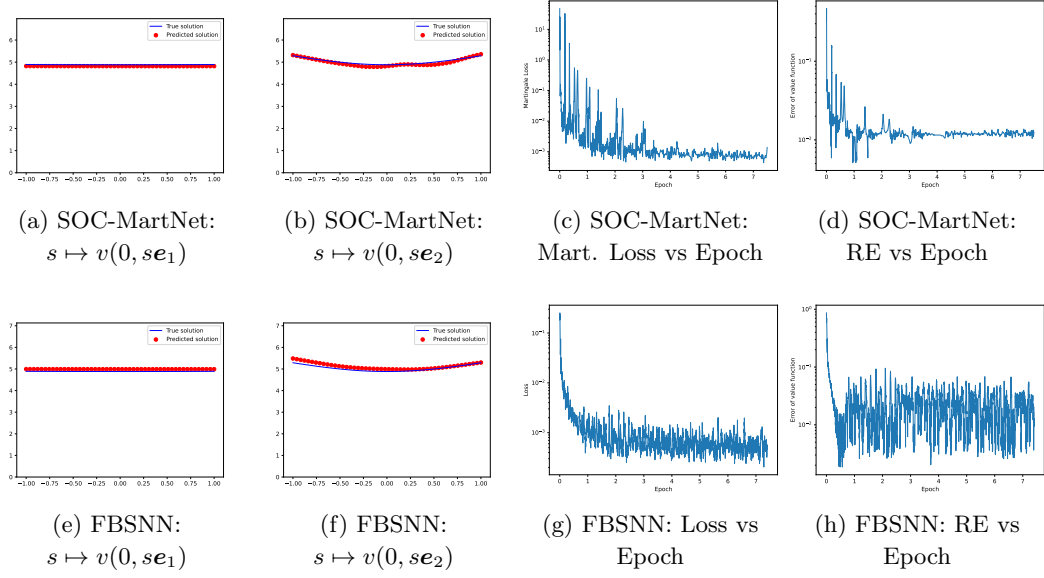


Figure 6: Numerical results for the semilinear parabolic problem (58) with $d = 50$ and smooth terminal function (60). The running times of SOC-MartNet and FBSNN are 16 and 122 seconds, respectively.

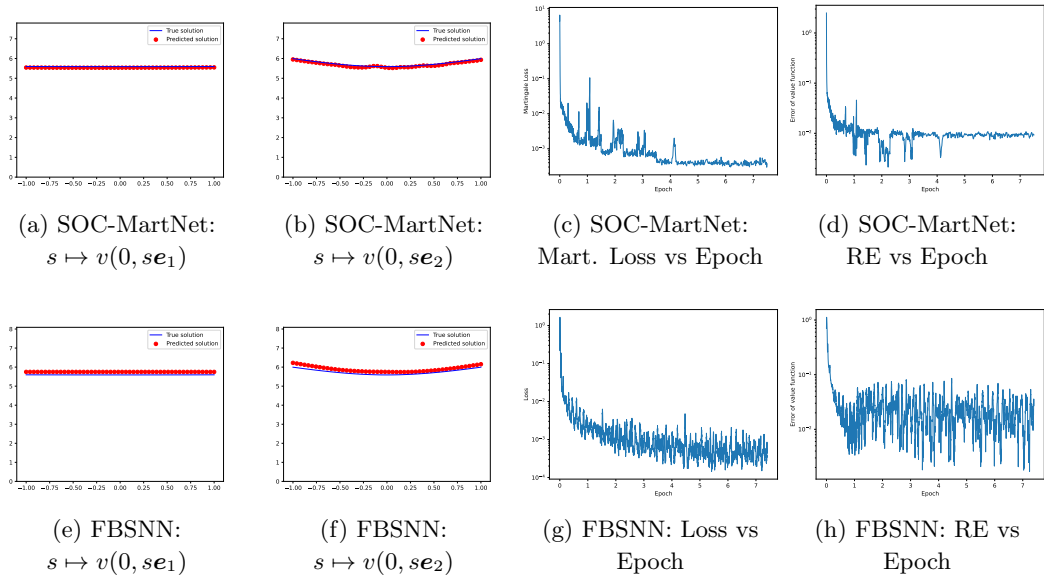


Figure 7: Numerical results for the semilinear parabolic problem (58) with $d = 100$ and smooth terminal function (60). The running times of SOC-MartNet and FBSNN are 22 and 120 seconds, respectively.

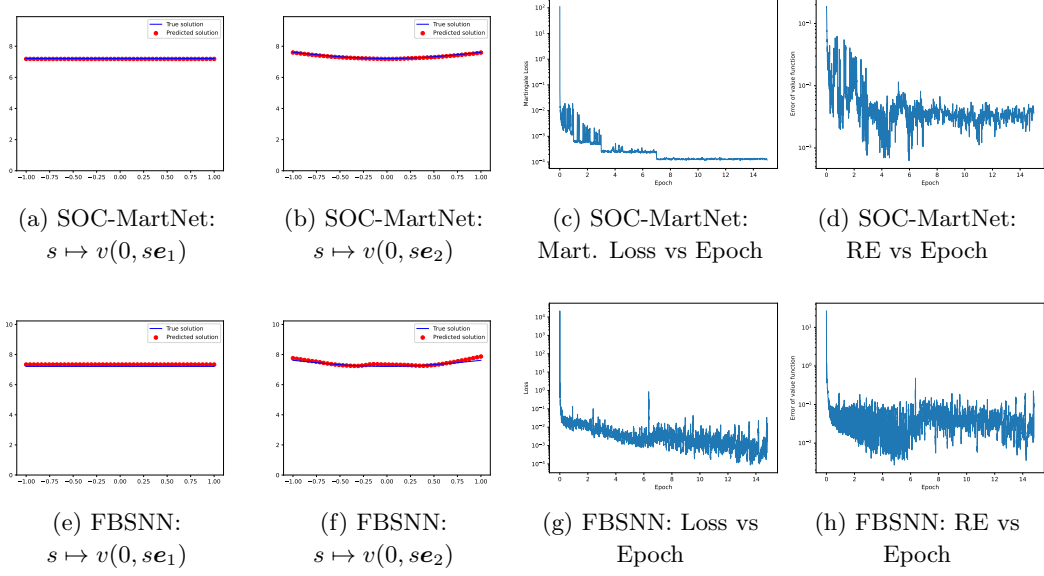


Figure 8: Numerical results for the semilinear parabolic problem (58) with $d = 500$ and smooth terminal function (60). The running times of SOC-MartNet and FBSNN are 269 and 305 seconds, respectively.

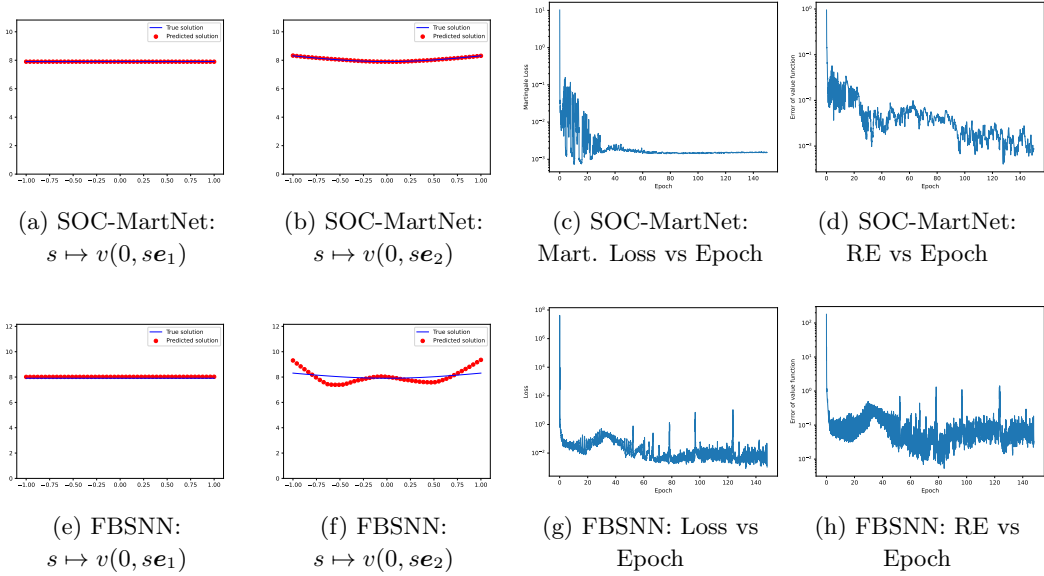


Figure 9: Numerical results for the semilinear parabolic problem (58) with $d = 1000$ and smooth terminal function (60). The running times of SOC-MartNet and FBSNN are 545 and 934 seconds, respectively.

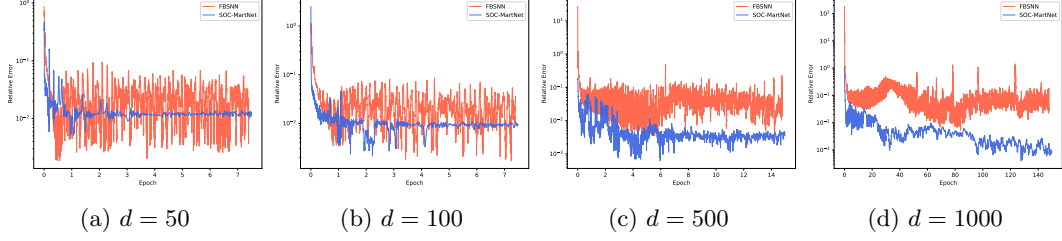


Figure 10: The RE vs Epoch for SOC-MartNet and FBSNN in solving the semilinear parabolic problem (58) with smooth terminal function (60).

4.2.2 Oscillatory terminal function

In the following, we consider an oscillatory terminal function as

$$g(x) := \frac{1}{d} \sum_{i=1}^d \left\{ \sin(x_i - \frac{\pi}{2}) + \sin\left((\delta + x_i^2)^{-1}\right) \right\}, \quad x \in \mathbb{R}^d, \quad \delta = \pi/10. \quad (61)$$

For this example, the true solution along the diagonal of the unite cube, i.e., $s \mapsto v(t, s\mathbf{e}_2)$, is independent of the spatial dimensionality d , whose graphs at $t = 0$ and T are presented in Figure 11. By Figure 11, although $s \mapsto v(T, s\mathbf{e}_2)$ is oscillatory around $s = 0$, the curve of $s \mapsto v(0, s\mathbf{e}_2)$ is relatively smooth and depends on the terminal time T . The relevant numerical results of SOC-MartNet (Algorithm 2) and FBSNN are presented in Figures 12 and 13.

Figure 12 demonstrates that the two methods remain unaffected by the oscillations in $g(x)$, and captures the analytical solution well. Moreover, the relative errors in Figure 13 show that the SOC-MartNet performs slightly better than the FBSNN.

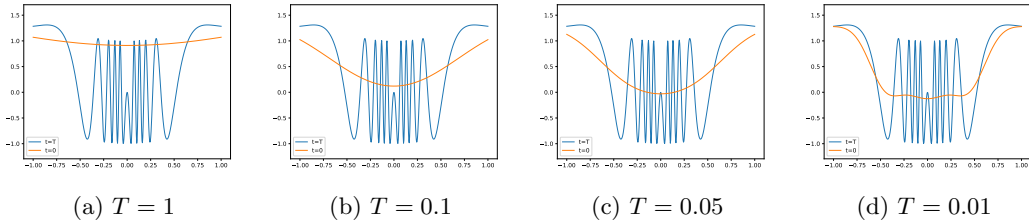


Figure 11: Graphs of the true solutions $s \mapsto v(t, s\mathbf{e}_2)$ of the semilinear parabolic problem (58) with a oscillatory terminal function (61) and with varying T .

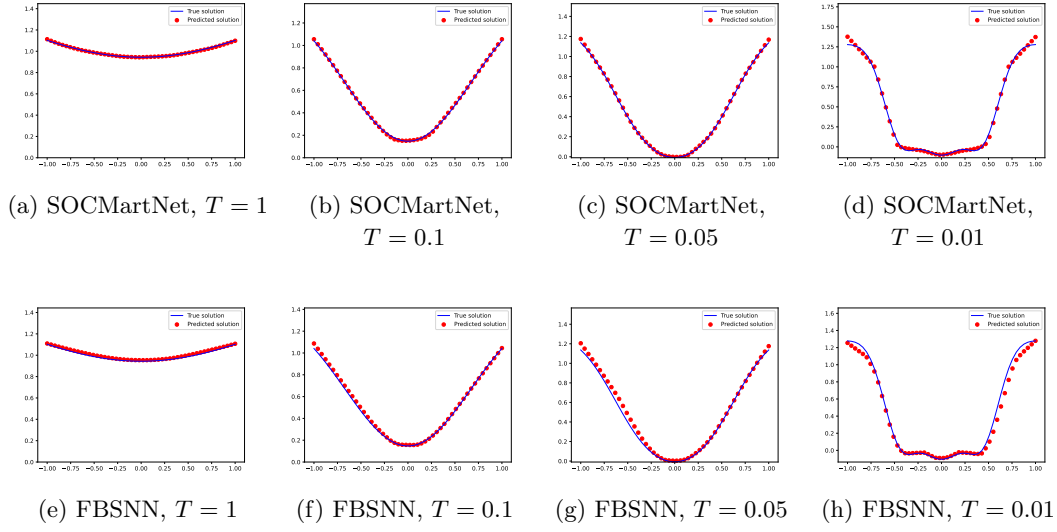


Figure 12: Graphs of the true solution and the numerical solution for $s \mapsto v(t, se_2)$ given by the semilinear parabolic problem (58) with $d = 100$ and oscillatory terminal function (61).

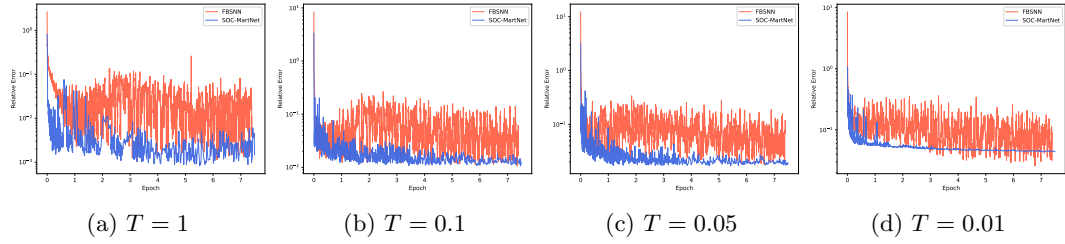


Figure 13: The RE vs Epoch for SOC-MartNet and FBSNN in solving the semilinear parabolic problem (58) with $d = 100$ and oscillatory terminal function (61).

4.3 Non-degenerated HJB equation without using explicit form of $\inf_u H$

We consider the following HJB equation from [1, Section 3.1]:

$$\begin{cases} (\partial_t + \Delta_x) v(t, x) + \inf_{\kappa \in \mathbb{R}^d} \left(2\kappa^\top \partial_x v(t, x) + |\kappa|^2 \right) = 0, & (t, x) \in [0, T] \times \mathbb{R}^d, \\ v(T, x) = 1 + g(x), & x \in \mathbb{R}^d. \end{cases} \quad (62)$$

The analytic solution of (62) is identical to (59). The HJB equation (62) is associated with the SOCP:

$$u^* = \arg \min_{u \in \mathcal{U}_{\text{ad}}} J(u), \quad J(u) := 1 + \mathbb{E} \left[\int_0^T |u_s|^2 ds + g(X_T^u) \right], \quad (63)$$

$$\mathcal{U}_{\text{ad}} = \left\{ u : [0, T] \times \Omega \rightarrow \mathbb{R}^d : u \text{ is } \mathbb{F}^B\text{-adapted} \right\}, \quad (64)$$

$$X_t^u = X_0 + \int_0^t 2u_s ds + \int_0^t \sqrt{2} dB_s, \quad t \in [0, T], \quad (65)$$

where B is a d -dimensional standard Brownian motion. The optimal feedback control is that

$$u^*(t, x) = -\partial_x v(t, x), \quad (t, x) \in [0, T] \times \mathbb{R}^d.$$

In this example, the HJB equation (62) is solved by the SOC-MartNet (Algorithm 1), where no explicit form is used for $\inf_{\kappa \in U} H$, and the optimal control u^* is approximated by u_α .

4.3.1 Smooth terminal function

We consider the HJB equation (62) with a smooth terminal function (60), of which the analytic solution is identical to the one considered in section 4.2.1. The relevant numerical results of the SOC-MartNet (Algorithm 1) are presented in Figures 14 to 18 and 20. As the numerical results show, despite not using the explicit form of $\inf_{\kappa \in U} H$, our SOC-MartNet still works well for the HJB equation with d upto 1000.

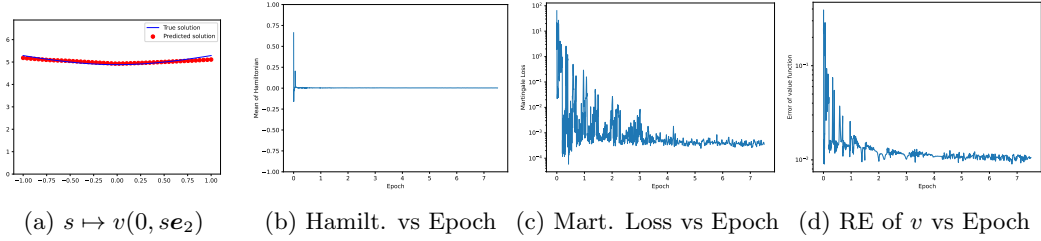


Figure 14: Numerical results of SOCMartNet for solving the HJB equation (62) with $d = 50$ and smooth terminal function (60).

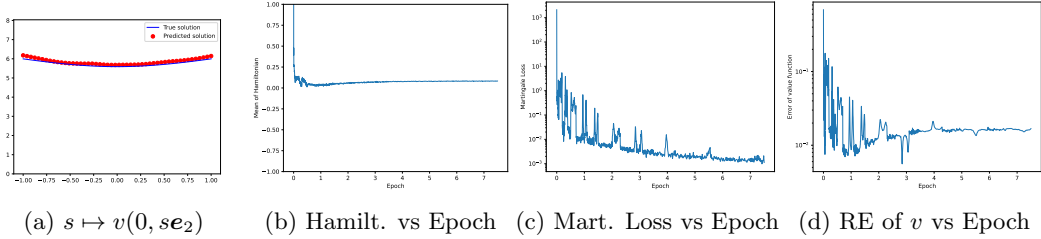


Figure 15: Numerical results of SOCMartNet for solving the HJB equation (62) with $d = 100$ and smooth terminal function (60).

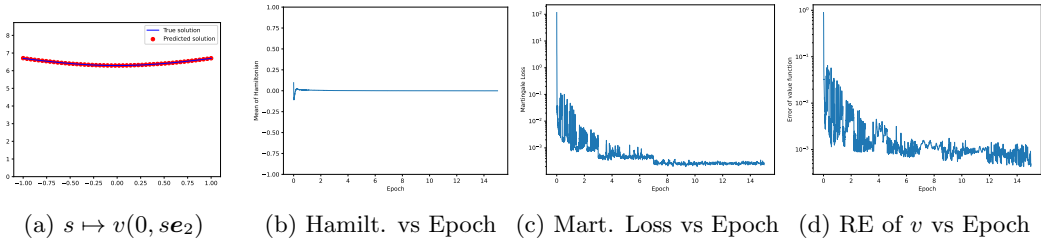


Figure 16: Numerical results of SOCMartNet for solving the HJB equation (62) with $d = 200$ and smooth terminal function (60).

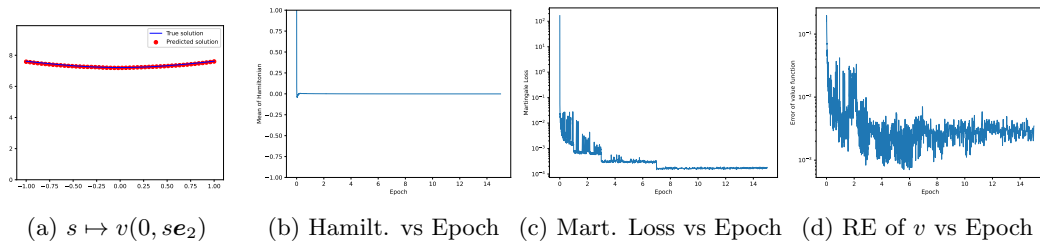


Figure 17: Numerical results of SOCMartNet for solving the HJB equation (62) with $d = 500$ and smooth terminal function (60).

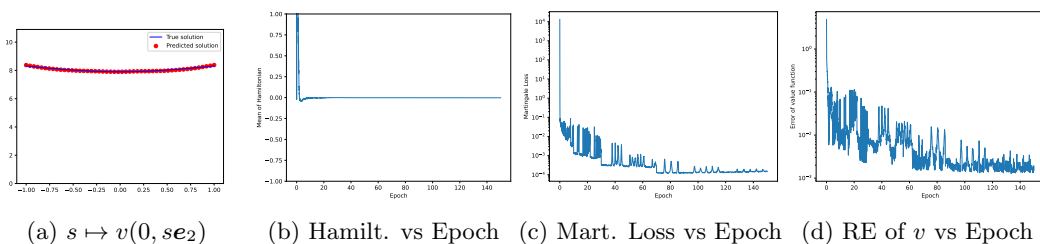


Figure 18: Numerical results of SOCMartNet for solving the HJB equation (62) with $d = 1000$ and smooth terminal function (60).

4.3.2 Oscillatory terminal function

In the following, we consider the HJB equation (62) with an oscillatory terminal function $g(x)$ defined in (61). The analytic solution is identical to the one presented in Figure 11. Numerical results in Figure 19 demonstrate that the SOC-MartNet maintains good performance for high-dimensional problems with oscillatory terminal functions.

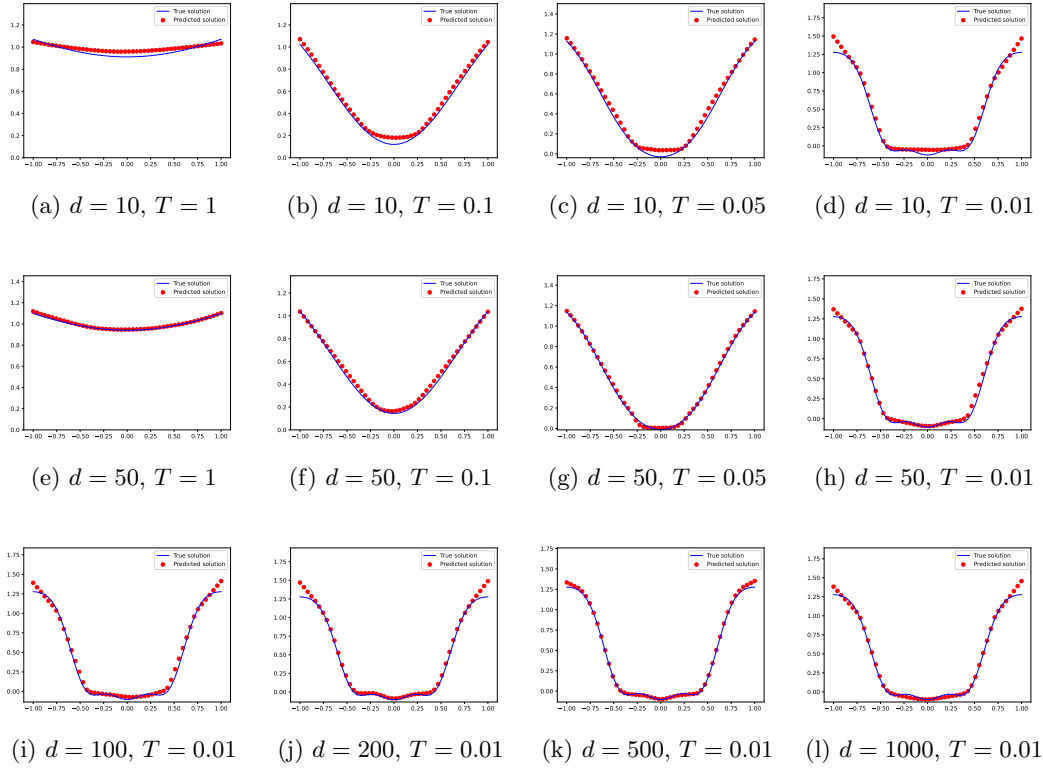


Figure 19: Graphs of the true solution and the numerical solution of SOC-MartNet for $s \mapsto v(t, se_2)$ at $t = 0$ given by the HJB equation (62) with oscillatory terminal function (61). The convergence history of the subplot (l) is presented in Figure 20.

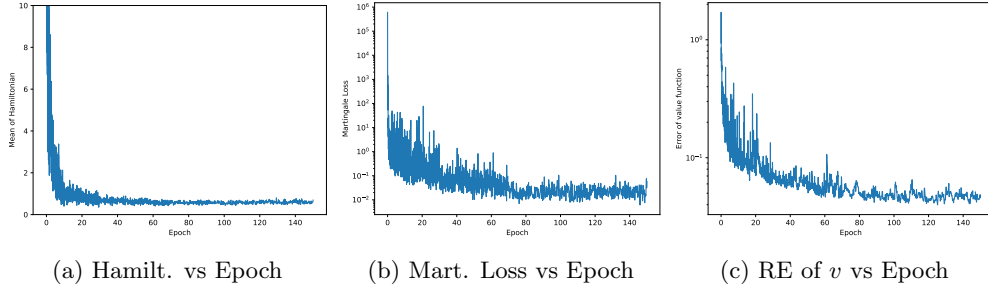


Figure 20: Convergence history for $d = 1000, T = 0.01$ of Figure 19(l).

4.3.3 Efficiency gain from DDP on multiple GPUs

To show the efficiency gain of our method from parallel computing, we apply the SOC-MartNet to the HJB equation (62) with a smooth terminal function (60). Table 1 shows the running times of Algorithm 1 using the strategy of DDP implemented on different numbers of GPUs. Notably, our SOC-MartNet can be accelerated significantly by the DDP, especially for the problem with dimensionality $d \geq 100$.

Table 1: RT of SOC-MartNet for solving (62) accelerated by DDP on multiple GPUs.
(unit: second)

GPUs	$d = 10$	$d = 50$	$d = 100$	$d = 500$	$d = 800$	$d = 1000$
$1 \times \text{V100}$	98	177	321	3049	7391	11332
$2 \times \text{V100}$	60	98	173	1548	3754	5692
$4 \times \text{V100}$	43	60	97	786	1898	2831
$8 \times \text{V100}$	41	44	63	407	974	1434

5 Conclusions

In this paper, we proposed a martingale based DNN method for stochastic optimal controls, SOC-MartNet, based on the original DeepMartNet [7; 8] combined with adversarial learning. A Hamiltonian process and a cost process are introduced using a control network and a value network. A loss function for the networks' training is used to ensure the minimum principle for the optimal feedback control as well as the fulfilment of the HJB equation by the value function, and the latter was implemented through a martingale formulation and a training that drives the value function network to satisfy its martingale properties at convergence. In SOC-MartNet, the martingale property of the cost process is however enforced by an adversarial learning, whose loss function is built upon the projection property of conditional expectations. Numerical results show that the proposed SOC-MartNet is effective and efficient for solving HJB-type equations with dimension up to 1000 in a small number of training epochs (less than 150), and particularly, for SCOPs where the $\inf H$ has no explicit expressions.

Acknowledgement

The authors thank Alain Bensoussan for helpful discussion on the HJB equation and stochastic optimal controls.

References

- [1] Achref Bachouch, Côme Huré, Nicolas Langrené, and Huyên Pham. Deep neural networks algorithms for stochastic control problems on finite horizon: numerical applications. *Methodol. Comput. Appl. Probab.*, 24(1):143–178, 2022.
- [2] Guy Barles and Espen Robstad Jakobsen. On the convergence rate of approximation schemes for Hamilton-Jacobi-Bellman equations. *M2AN Math. Model. Numer. Anal.*, 36(1):33–54, 2002.
- [3] R. W. Beard, G. N. Saridis, and J. T. Wen. Approximate solutions to the time-invariant Hamilton-Jacobi-Bellman equation. *J. Optim. Theory Appl.*, 96(3):589–626, 1998.
- [4] Randal W. Beard, George N. Saridis, and John T. Wen. Galerkin approximations of the generalized Hamilton-Jacobi-Bellman equation. *Automatica J. IFAC*, 33(12):2159–2177, 1997.

- [5] Richard Bellman. *Dynamic programming*. Princeton University Press, Princeton, NJ, 1957.
- [6] Simone Cacace, Emiliano Cristiani, Maurizio Falcone, and Athena Picarelli. A patchy dynamic programming scheme for a class of Hamilton-Jacobi-Bellman equations. *SIAM J. Sci. Comput.*, 34(5):A2625–A2649, 2012.
- [7] Wei Cai. DeepMartNet – a martingale based deep neural network learning algorithm for eigenvalue/BVP problems and optimal stochastic controls, 2023, arXiv:2307.11942 [math.NA].
- [8] Wei Cai, Andrew He, and Daniel Margolis. DeepMartNet – a martingale based deep neural network learning method for Dirichlet BVP and eigenvalue problems of elliptic pdes, 2023, arXiv:2311.09456 [math.NA].
- [9] Michael G. Crandall, Hitoshi Ishii, and Pierre-Louis Lions. User’s guide to viscosity solutions of second order partial differential equations. *Bull. Amer. Math. Soc. (N.S.)*, 27(1):1–67, 1992.
- [10] Michael G. Crandall and Pierre-Louis Lions. Viscosity solutions of Hamilton-Jacobi equations. *Trans. Amer. Math. Soc.*, 277(1):1–42, 1983.
- [11] Jérôme Darbon, Gabriel P. Langlois, and Tingwei Meng. Overcoming the curse of dimensionality for some Hamilton-Jacobi partial differential equations via neural network architectures. *Res. Math. Sci.*, 7(3):Paper No. 20, 50, 2020.
- [12] Jérôme Darbon and Tingwei Meng. On some neural network architectures that can represent viscosity solutions of certain high dimensional Hamilton-Jacobi partial differential equations. *J. Comput. Phys.*, 425:Paper No. 109907, 16, 2021.
- [13] Sergey Dolgov, Dante Kalise, and Karl K. Kunisch. Tensor decomposition methods for high-dimensional Hamilton-Jacobi-Bellman equations. *SIAM J. Sci. Comput.*, 43(3):A1625–A1650, 2021.
- [14] Weinan E, Jiequn Han, and Arnulf Jentzen. Deep learning-based numerical methods for high-dimensional parabolic partial differential equations and backward stochastic differential equations. *Commun. Math. Stat.*, 5(4):349–380, 2017.
- [15] Weinan E, Jiequn Han, and Arnulf Jentzen. Algorithms for solving high dimensional PDEs: from nonlinear Monte Carlo to machine learning. *Nonlinearity*, 35(1):278–310, 2022.
- [16] Wendell H. Fleming and Raymond W. Rishel. *Deterministic and stochastic optimal control*, volume No. 1 of *Applications of Mathematics*. Springer-Verlag, Berlin-New York, 1975.
- [17] Yu Fu, Weidong Zhao, and Tao Zhou. Highly accurate numerical schemes for stochastic optimal control via FBSDEs. *Numer. Math. Theory Methods Appl.*, 13(2):296–319, 2020.
- [18] Jean-François Le Gall. *Brownian Motion, Martingales, and Stochastic Calculus*. Springer Cham, 2016.

- [19] Zhiwei Gao, Liang Yan, and Tao Zhou. Failure-informed adaptive sampling for PINNs. *SIAM J. Sci. Comput.*, 45(4):A1971–A1994, 2023.
- [20] Bo Gong, Wenbin Liu, Tao Tang, Weidong Zhao, and Tao Zhou. An efficient gradient projection method for stochastic optimal control problems. *SIAM J. Numer. Anal.*, 55(6):2982–3005, 2017.
- [21] Ling Guo, Hao Wu, Xiaochen Yu, and Tao Zhou. Monte Carlo fPINNs: deep learning method for forward and inverse problems involving high dimensional fractional partial differential equations. *Comput. Methods Appl. Mech. Engrg.*, 400:Paper No. 115523, 17, 2022.
- [22] Jiequn Han and Weinan E. Deep learning approximation for stochastic control problems. *Deep Reinforcement Learning Workshop, NIPS*, 2016, arXiv:1611.07422 [cs.LG].
- [23] Z. Hu, K. Shukla, GE. Karniadakis, K. Kawaguchi K. Tackling the curse of dimensionality with physics-informed neural networks. *Neural Networks*, 176:106369, 2024.
- [24] Côme Huré, Huyên Pham, Achref Bachouch, and Nicolas Langrené. Deep neural networks algorithms for stochastic control problems on finite horizon: convergence analysis. *SIAM J. Numer. Anal.*, 59(1):525–557, 2021.
- [25] Côme Huré, Huyên Pham, and Xavier Warin. Deep backward schemes for high-dimensional nonlinear PDEs. *Math. Comp.*, 89(324):1547–1579, 2020.
- [26] Hitoshi Ishii. On uniqueness and existence of viscosity solutions of fully nonlinear second-order elliptic PDEs. *Comm. Pure Appl. Math.*, 42(1):15–45, 1989.
- [27] Robert Jensen. The maximum principle for viscosity solutions of fully nonlinear second order partial differential equations. *Arch. Rational Mech. Anal.*, 101(1):1–27, 1988.
- [28] Shaolin Ji, Shige Peng, Ying Peng, and Xichuan Zhang. Solving stochastic optimal control problem via stochastic maximum principle with deep learning method. *J. Sci. Comput.*, 93(1):Paper No. 30, 28, 2022.
- [29] Dante Kalise and Karl Kunisch. Polynomial approximation of high-dimensional Hamilton-Jacobi-Bellman equations and applications to feedback control of semi-linear parabolic PDEs. *SIAM J. Sci. Comput.*, 40(2):A629–A652, 2018.
- [30] Wei Kang and Lucas C. Wilcox. Mitigating the curse of dimensionality: sparse grid characteristics method for optimal feedback control and HJB equations. *Comput. Optim. Appl.*, 68(2):289–315, 2017.
- [31] Idris Kharroubi, Nicolas Langrené, and Huyên Pham. A numerical algorithm for fully nonlinear HJB equations: an approach by control randomization. *Monte Carlo Methods Appl.*, 20(2):145–165, 2014.
- [32] Idris Kharroubi, Nicolas Langrené, and Huyên Pham. Discrete time approximation of fully nonlinear HJB equations via BSDEs with nonpositive jumps. *Ann. Appl. Probab.*, 25(4):2301–2338, 2015.

- [33] Idris Kharroubi and Huyên Pham. Feynman-Kac representation for Hamilton-Jacobi-Bellman IPDE. *Ann. Probab.*, 43(4):1823–1865, 2015.
- [34] Achim Klenke. *Probability Theory*. Springer Cham, third edition, 2020.
- [35] N. V. Krylov. *Controlled diffusion processes*, volume 14 of *Applications of Mathematics*. Springer-Verlag, New York-Berlin, 1980. Translated from the Russian by A. B. Aries.
- [36] N. V. Krylov. *Nonlinear elliptic and parabolic equations of the second order*, volume 7 of *Mathematics and its Applications (Soviet Series)*. D. Reidel Publishing Co., Dordrecht, 1987. Translated from the Russian by P. L. Buzytsky [P. L. Buzytskiĭ].
- [37] K. Kunisch, S. Volkwein, and L. Xie. HJB-POD-based feedback design for the optimal control of evolution problems. *SIAM J. Appl. Dyn. Syst.*, 3(4):701–722, 2004.
- [38] Pierre-Louis Lions. *Generalized solutions of Hamilton-Jacobi equations*, volume 69 of *Research Notes in Mathematics*. Pitman (Advanced Publishing Program), Boston, Mass.-London, 1982.
- [39] Tenavi Nakamura-Zimmerer, Qi Gong, and Wei Kang. Adaptive deep learning for high-dimensional Hamilton-Jacobi-Bellman equations. *SIAM J. Sci. Comput.*, 43(2):A1221–A1247, 2021.
- [40] Carmeliza Navasca and Arthur J. Krener. Patchy solutions of Hamilton-Jacobi-Bellman partial differential equations. In *Modeling, estimation and control*, volume 364 of *Lect. Notes Control Inf. Sci.*, pages 251–270. Springer, Berlin, 2007.
- [41] Bernt Øksendal. *Stochastic differential equations*. Universitext. Springer-Verlag, Berlin, sixth edition, 2003. An introduction with applications.
- [42] S Osher and CW Shu. High-order essentially nonoscillatory schemes for hamilton-jacobi equations. *SIAM Journal on numerical analysis*, 4:907–922, 1991.
- [43] Huyên Pham. *Continuous-time stochastic control and optimization with financial applications*, volume 61 of *Stochastic Modelling and Applied Probability*. Springer-Verlag, Berlin, 2009.
- [44] M. Raissi, P. Perdikaris, and G. E. Karniadakis. Physics-informed neural networks: a deep learning framework for solving forward and inverse problems involving nonlinear partial differential equations. *J. Comput. Phys.*, 378:686–707, 2019.
- [45] S. Richardson and S. Wang. Numerical solution of Hamilton-Jacobi-Bellman equations by an exponentially fitted finite volume method. *Optimization*, 55(1-2):121–140, 2006.
- [46] Iain Smears and Endre Süli. Discontinuous Galerkin finite element approximation of Hamilton-Jacobi-Bellman equations with Cordes coefficients. *SIAM J. Numer. Anal.*, 52(2):993–1016, 2014.

- [47] S. Wang, L. S. Jennings, and K. L. Teo. Numerical solution of Hamilton-Jacobi-Bellman equations by an upwind finite volume method. volume 27, pages 177–192. 2003. International Workshop on Optimization with High-Technology Applications (OHTA 2000) (Hong Kong).
- [48] Jiongmin Yong and Xun Yu Zhou. *Stochastic controls*, volume 43 of *Applications of Mathematics (New York)*. Springer-Verlag, New York, 1999. Hamiltonian systems and HJB equations.
- [49] Yaohua Zang, Gang Bao, Xiaojing Ye, and Haomin Zhou. Weak adversarial networks for high-dimensional partial differential equations. *J. Comput. Phys.*, 411:109409, 14, 2020.
- [50] Wenzhong Zhang and Wei Cai. FBSDE based neural network algorithms for high-dimensional quasilinear parabolic PDEs. *J. Comput. Phys.*, 470:Paper No. 111557, 14, 2022.
- [51] Weidong Zhao, Tao Zhou, and Tao Kong. High order numerical schemes for second-order FBSDEs with applications to stochastic optimal control. *Commun. Comput. Phys.*, 21(3):808–834, 2017.
- [52] Mo Zhou, Jiequn Han, and Jianfeng Lu. Actor-critic method for high dimensional static Hamilton-Jacobi-Bellman partial differential equations based on neural networks. *SIAM J. Sci. Comput.*, 43(6):A4043–A4066, 2021.